LETTER

Meso-porous membrane of noble metal for surface plasmon resonance gas sensors

Takayuki Numata · Yukitoshi Otani ·
Norihiro Umeda

Since surface plasmon resonance (SPR) provides quick response and high sensitivity to environmental substances, it is recognized as a powerful technique for toxic gas detection system [1–3]. Although already reported SPR gas sensors have achieved a high sensitivity at the ppm level, the adsorption of vapor molecules relies only on the affinity of the planar surface of the sensitive membrane. In terms of adsorption efficiency, a planar adsorber element is less advantageous because the specific surface area is small. It is expected that the sensitivity of the SPR gas sensor could be improved by introducing a porous structure to the sensor surface. However, in order to excite SPR at optical frequencies, materials are limited to Ag or Au on account of the dielectric permittivity to achieve wavenumber matching. These noble metals are stable both chemically and physically, and fabrication of a nano-sized porous structure on these metals has been difficult.

In this letter, a meso-porous membrane of a noble metal on which SPR can be excited is reported. The adsorption of water vapor on the membrane is observed from the SPR signal, and the dimension of the porous structure is validated by the Kelvin's capillary condensation theory.

The meso-porous structure proposed in this study is based on the surface profile of a two-dimensional colloidal crystalline structure (CCS) of mono-sized nanoparticles. By utilizing this as a substrate for metallic vapor deposition, a metal film with a surface profile consisting of a number of nano-sized pores and grooves is realized. The crystalline structure is fabricated utilizing the self-assembling behavior of colloidal polymer nanoparticles spread on a hydrophilic glass slide [4]. First, a glass slide is washed carefully with a sponge containing surfactant, and then rinsed couple of times with pure water and organic solvent for degreasing. After rinsing, it is dried by blowing N_2 gas over it. Due to the cleaning, the surface of the glass slide obtains a hydrophilic property. In the next stage, a colloidal aqueous solution of polystyrene nanospheres is dropped onto the cleaned surface of the stationary glass slide. As the thickness of the suspension layer becomes smaller than the diameter of the colloidal particles, owing to the evaporation, the particles are forced to attract each other due to capillary force. When the solvent is completely evaporated, the particles form a closely packed hexagonal crystalline structure on the surface of the glass slide.

The crystalline structure of the nanoparticles intrinsically possesses nano-sized grooves and cavities of high aspect ratio at the interface of constitutive particles. As illustrated in Fig. 1a, each particle in the crystalline structure has contact points with the neighboring particles every 60° of the azimuth angle. The cross-sectional profile of the contact point of the two particles, expressed by the line A–B, shows a cycloidal surface profile as depicted in Fig. 1b. The width of the wedge-shaped groove gradually decreases and finally becomes zero numerically in the limit. This means that an ultimate porous structure is realized at the contact points. In addition, a small quasi-triangular cavity is

T. Numata (✉) · Y. Otani · N. Umeda
Faculty of Engineering, Tokyo University of Agriculture
and Technology, Nakacho 2-24-16, Koganei,
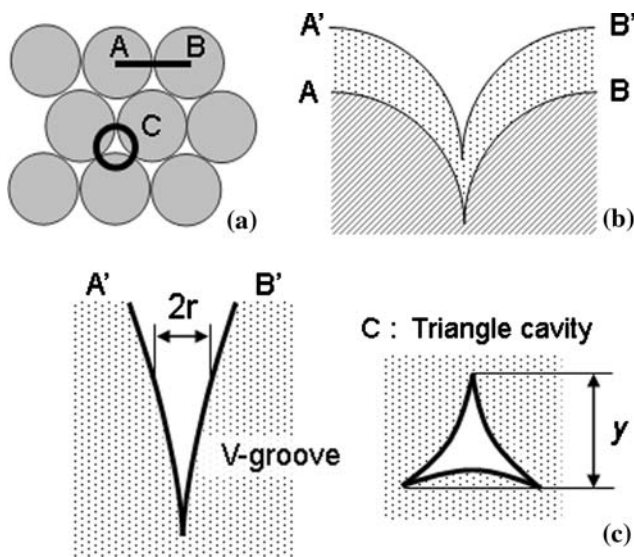Tokyo 184-8588, Japan
e-mail: t-numata@cc.tuat.ac.jp

Fig. 1 (**a**) An overview of the two-dimensional CCS of the nanoparticles. (**b**) Schematic diagram of cycloidal surface profile of the CCS (cross-section: A–B) and deposited metal layer tracing the CCS profile as A′–B′. (**c**) Geometric profiles of the porous structure on the membrane

Fig. 2 (**a**) A schematic cross-section diagram of the fabricated membrane. (**b**) Topography of the fabricated Ag membrane based on 356 nm diameter particles taken by AFM

also formed in the region enclosed by three neighboring particles as indicated by the circle C. The dimensions of the cavity can be geometrically calculated from the size of the constitutive particle [5]. For instance, 46 nm of y is obtained from a structure with 200 nm diameter particles. Therefore, nano-sized pores are periodically provided through-out the substrate with CCS. Vertical deposition of a collimated metallic vapor over the CCS substrate allows production of a periodic metal meso-porous structure tracing the surface profile of CCS, as illustrated in Fig. 1c. In principle, the method of creating a nanostructure proposed here can be applied to various kinds of metal. In this study, Ag is employed to excite SPR. In the experiment, the deposition was obtained by resistance-heating physical vapor deposition (PVD) process. The 1×1 cm^2 CCS substrate was set to face the vapor source with a separation distance of 15 cm. As a result, nearly collimated vapor is incident vertically on whole area of CCS surface. Figure 2a, b shows a schematic cross-sectional structure of the membrane and the topography of the deposited Ag layer obtained by an atomic force microscope (AFM), respectively. The fundamental surface profile of the CCS is definitely traced by the deposited layer. In this study, test membranes were fabricated with 202 and 356 nm diameter polystyrene particles. The thicknesses of deposited metal layer were 96 and 89 nm for 202 and 356 nm CCS substrates, respectively. Topographic inspection using AFM
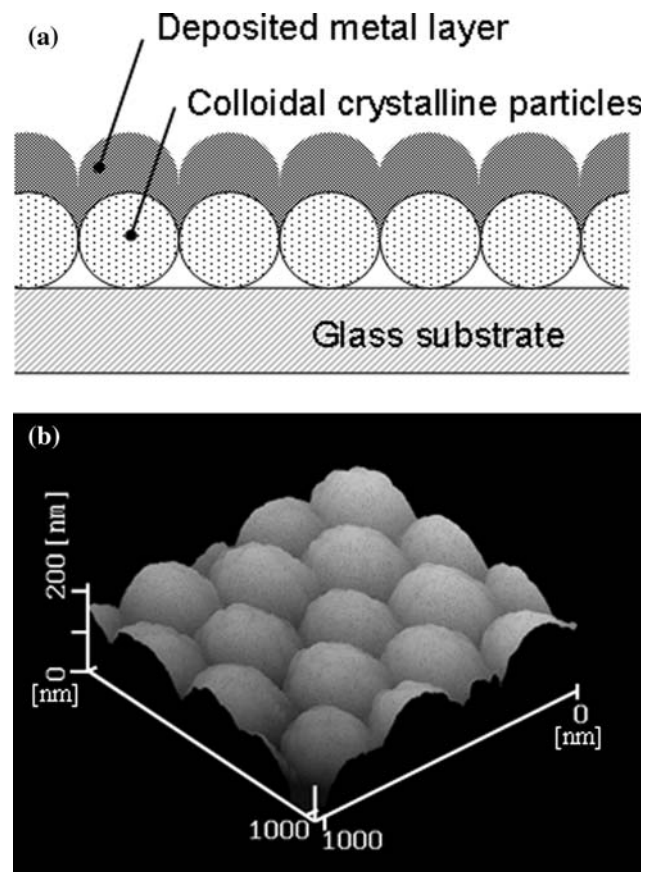
showed the variation in deposition thickness on an individual substrate was less than ±2 nm and ensured high uniformity of the deposited layer. The fabricated Ag layer had a continuous and cycloidal periodicity in its surface profile as well as a number of nano-sized grooves and cavities. On such a periodic nanostructure of a noble metal, the SPR can be excited by the diffraction component of incident light [6–8]. In the case of white light illumination, a partial wave component consumed to excite SPR is adsorbed into the metal, which produces a dip in the specular reflection spectrum. In the experiment, the excitation of SPR on the fabricated membrane was verified by observing its specular reflection spectrum with illumination of p-polarized white light at an incidence angle of 35°. The probing white light was focused and illuminated the surface of fabricated porous structure with a spot diameter of around 150 μm to perform a close investigation and enhance the accuracy of measurement.

In order to evaluate the dimension of porous structure, the adsorption of water vapor on the Ag

membrane was investigated through the SPR signal. As a preparation, the surface of the deposited Ag was oxidized by dipping it into a dilute H_2O_2 solution to form surface hydroxyl groups which provide physisorption sites for environmental vapor molecules. In the experiment, the accumulation of adsorbed water molecules due to the temperature of the membrane was monitored through the change in SPR signal under a static environmental vapor pressure. Figure 3a, b represents the normalized absorbance of the fabricated membranes due to the temperature. The environmental relative humidity and temperature were 64.4%, 25.6 °C and 63.2%, 25.5 °C for 202 and 356 nm membranes, respectively. The peak absorbance in each curve differed due to the periodic geometry of the membranes, showing an excitation of SPR by diffraction coupling. The curves exhibit red shift with decreasing temperature. As the temperature of the membrane decreases, vapor molecules near its surface are deprived of their thermodynamic energy, and are then bound onto the surface hydroxyl groups. In both cases, the red shift of the absorbance curve stops as the surface of the porous membrane is filled with adsorbed water, in spite of further accumulation of molecules. This is attributed to the fact that the thickness of the adsorbed layer which interacts with SPR is limited to several hundred nanometers from the metal surface.

The relationship between the shift and the temperature can be recognized as an adsorption isobar for the fabricated porous membrane. Figure 4 shows the shift in the wavelength of the absorbance peak due to the temperature of the membrane. The major shift initiates when the temperature reaches around 22 °C on both membranes, whereas little change can be observed at higher temperatures. In principle, the shift of the absorbance curve indicates a change in dielectric permittivity owing to additional molecular adsorption and capillary condensation on the porous membrane [9]. Therefore, the size of the pore structure can be estimated by using Kelvin's capillary condensation theory. The physical behavior of vapor molecules and their condensation inside a small pore is described by Kelvin's equation as

$$\ln\left(\frac{p}{p_s}\right) = \frac{V\gamma\cos\theta}{rRT}, \qquad (1)$$

where (p/p_s) is the ratio of partial pressure of a gas to its saturation pressure. V, γ, and θ represent the molecular mass, the surface tension, and the contact angle with the pore wall of the condensed matter, respectively. Denominators, r, R, and T are the radius
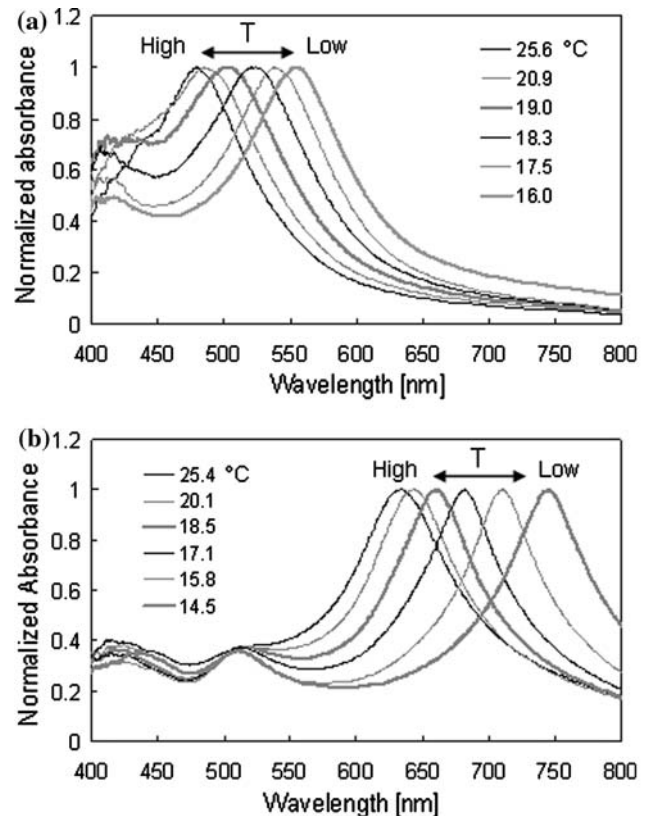

Fig. 3 Specular-reflection absorbance spectra of fabricated Ag membranes with 202 nm diameter particles (**a**) and 356 nm diameter particles (**b**). Each spectrum makes a redshift according to the adsorption of vapor molecules
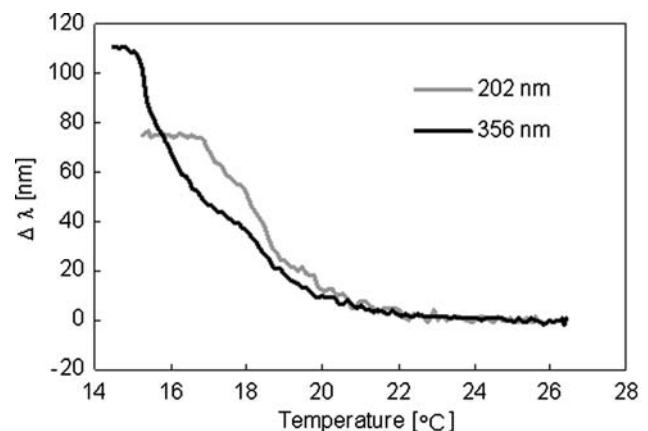

Fig. 4 SPR signal-based adsorption isobars of fabricated membranes. Major adsorption initiates at temperatures higher than the theoretical dew point owing to capillary condensation at nano-sized porous structure

of the pore, the gas constant, and absolute temperature, respectively. The equation indicates that the saturation vapor pressure in a small pore is less than that of the bulk phase. From Eq. 1, using experimentally obtained

parameters, with condensation at 22 °C in 64% RH environment, the radius of the pores was estimated to be ~2.4 nm. As shown in Fig. 4, both 202 and 356 nm membranes exhibited similar initial adsorbance temperatures which were higher than the theoretical dew point. This suggests that the v-shaped grooves between each particle have mainly contributed to the initial condensation of vapor to enhance the adsorption efficiency, rather than the triangular cavities which directly depend on the size of the CCS particles. In addition, it is confirmed that the adsorption efficiency of the membrane has been significantly enhanced by the structure of the pore. Other differences in adsorption curves, inclination or saturation value, may be attributed to the difference in the membrane structure, such as the specific area of the membrane surface. Nonetheless, the results indicate that the proposed technique might be effective especially for detecting very low concentrations of gaseous substances in the environment. Although the size of the pores becomes numerically zero at the contact point of each particle, practically, it is a finite size. This is attributed to the incompletely collimated metallic vapor due to the thermal diffusion in the PVD process, which prevents the deposited layer from tracing the surface profile on the CCS with a high aspect ratio. In this technique, thickness of the deposition layer is also an essential parameter for creation of porous structure. Excess deposition leads filling up of the grooves and cavities on CCS and degrades the gas detection sensitivity. On the other hand, smaller thickness gives shallower grooves. However, a shortage of thickness makes the metal layer discontinuous and seriously affects excitation condition of SPR. Therefore, appropriate control of deposition thickness is necessary to obtain an ideal membrane structure. Collimation of vapor and appropriate deposition thickness will provide smaller pores, and thus, further enhancement of the adsorption efficiency.

References

1. Liedberg B, Nylander C, Lundstrom I (1983) Sens Actuators 4:299
2. Nylander C, Liedberg B, Lind T (1982/83) Sens Actuators 3:79
3. Samoylov AV, Mirsky VM, Hao Q, Swart C, Shirshov Y, Wolfbeis OS (2005) Sens Actuators B 106:369
4. Fischer UC, Zingsheim HP (1981) J Vac Sci Technol 19:881
5. Hulteen JC, Van Duyne RP (1994) Vac Sci Technol A 13:1553
6. Raether H (1988) Surface plasmons on smooth and rough surfaces and on gratings. Springer-Verlag, Berlin, Chapter 2
7. Homola J (2003) Anal Bioanal Chem 377:528
8. Kano H, Kawata S (1995) Jpn J Appl Phys 34:331
9. Talmachev VA (2001) J Opt Technol 68:328